Influence of residual stresses on fatigue crack propagation

S. SIRTORI, L. VERGANI, Dipartimento di Meccanica, Politecnico di Milano.

Abstract

An examination is made of the influence of a compression self-stresses field on the fatigue crack propagation.
CT test specimens made of SA 533 were subjected to the same variable, constant-amplitude load. The ratio between the minimum and maximum stress was R = 0.1.
Some specimens had been previously subjected to a pulsating load to cause plastic straining in the maximum stress zone, so as to set up a field of residual stresses. The pattern and values of the residual stresses were determined experimentally by means of electrical strain gauges suitably located on the surfaces of the specimens.
Pari's equation was used for theoretical analysis of the results.
A closer resemblance to reality was observed in the specimens with residual stresses when the effective stress intensity factor (sum of the contributions of the applied and the residual stresses) and the effective ratio R were taken into consideration.

Riassunto

Influenza degli sforzi residui sulla propagazione delle cricche di fatica

In questo lavoro si è studiata l'influenza che un campo di autotensioni, di compressione all'apice della cricca, esercita sulla propagazione di quest'ultima a fatica.
Sono stati utilizzati dei provini CT, costruiti con materiale SA 533 e sottoposti tutti allo stesso carico variabile ad ampiezza costante e con un rapporto fra lo sforzo minimo e lo sforzo massimo R = 0,1.
Alcuni dei provini in precedenza erano già stati sottoposti ad un carico pulsante, tale da provocare una plasticizzazione del materiale, nella zona dove si verificano gli sforzi massimi, e quindi da instaurare un campo di autotensioni. L'andamento e i valori degli sforzi residui sono stati rilevati sperimentalmente tramite degli estensimetri elettrici, opportunamente posizionati sulle facce dei provini.
L'analisi teorica dei risultati è stata eseguita utilizzando l'equazione di Paris.
Si è riscontrata una maggiore aderenza alla realtà nel caso dei provini con tensioni residue, considerando l'effettivo fattore di intensità degli sforzi, dato dalla somma dei contributi dovuti sia allo sforzo applicato sia alle autotensioni, e l'effettivo rapporto sforzo minimo/sforzo massimo R.

Introduction

Machine members are often subjected to self-stresses derived, for example, from the technological processes used in their forming and heat treatments, or thermic gradient and local plasticisation because of overloading and stress concentration in notched zones.

The strong influence of residual stresses on fatigue crack propagation has received considerable attention in the literature (1-8), especially with regard to the opposite effects of residual compression and traction stresses on the propagation rate. The former, in fact, are accompanied by slower rate, whereas faster rate is observed when a field of residual traction stresses is present. The possible existence of residual stresses must thus be taken into account when fatigue crack propagation predictions are to be accurately estimated.

Two approaches are usually employed for this purpose:

a) superposition of stress intensity factors embracing both the applied and residual stresses.

b) examination of models in which provision is made for crack closure.

This paper describes experimental tests carried out to evaluate the growth rate of a crack in the presence of a field of compression self-stresses, using approach a) for the theoretical assessment of their effects.

Experimental test

CT test specimens of uniform size were prepared. On some specimens, a hole with radius r = 4 mm was made at the tip of the notch. It was positioned in such a way as not to alter the area of the resistent section of the specimen (see Fig. 1).

Fig. 1 - CT test specimens with (b) and without (a) holes. Specimens (b) were subjected to a pulsed load designed to set up a field of internal compression tensions at the crack tip.

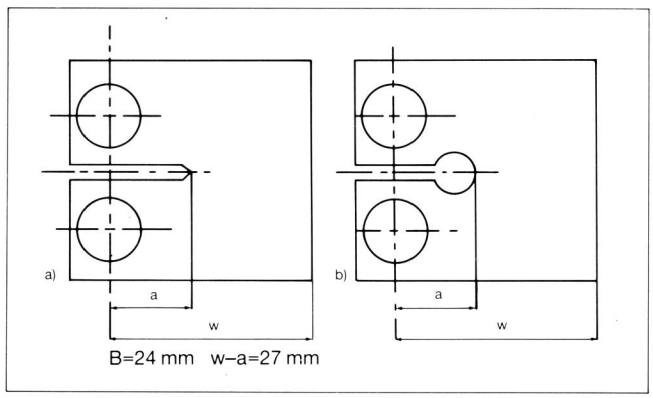

The material employed (SA 533) has the following strength characteristics:

$R_{eL} = 560$ N/mm^2
$R_m = 680$ N/mm^2
$A = 16\%$
$Z = 75\%$
$E = 211.000$ N/mm^2
$\alpha = 0.27$

$\sigma - \varepsilon$ curves for SA 533 derived from classic traction test specimens and from the literature data (10) are set out in Fig. 2.

Annex A describes the method used and the values obtained for the cyclic curve.
The Paris equation for the specimens without a hole was:

$$\frac{da}{dN} = C\,(\Delta k)^n$$

using R = 0.1 and applied load ΔP = 11,250 N
Crack propagation was measured with crack gage and a 50 x light microscope on both surfaces of the test specimen.

A check was carried out on all specimens to make sure that the configuration of the cracks within their thickness was not such as to require any correction for crack deviation.
The stress intensity factor ΔK was derived from the following equation:

$$\Delta K = \frac{\Delta P}{BW}\,\frac{(2+\alpha)}{(1-\alpha)^{3/2}}\cdot(0{,}866 + 4{,}64\alpha - 13{,}32\alpha^2 + 14{,}72\alpha^3 - 5{,}6\alpha^4)$$

Fig. 2 - Characteristic curves for SA 533.
a) Traction curve; b) Cyclic curve.

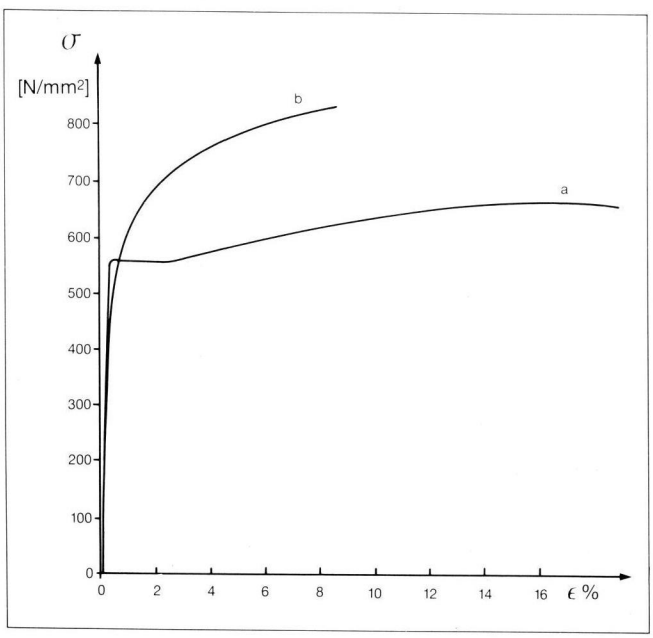

where:

P = load applied

B = thickness of the specimen
W = width of the specimen
α = a/w
a = distance of load application axis from the crack tip.

The specimens with holes were subjected to a pulsed load P = 0-40,000 N.

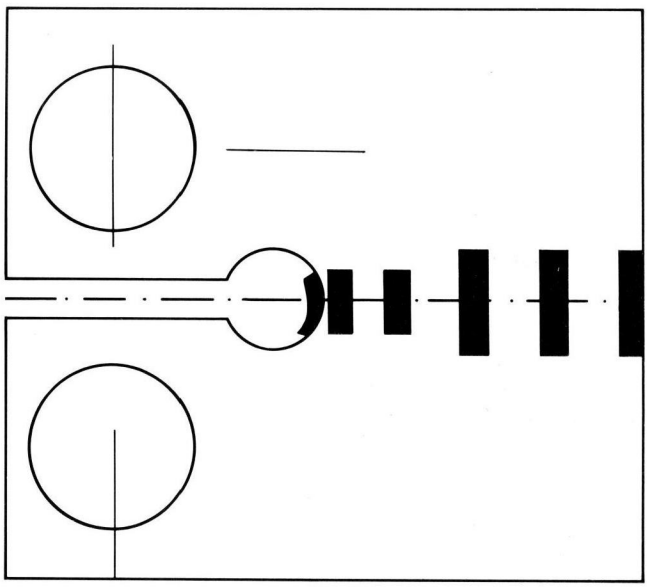

Fig. 3 - Location of the electrical strain gauges on the specimen surfaces for the measurement of residual strains.

The presence of the hole permitted the positioning of two electrical strain gauges (measurement base: 0.6 mm) in the point of maximum stress (one on each face), so as to detect the nucleation of the fatigue crack; this occured after about N = 12,000 load cycles.

The load applied was such as to cause plasticisation of the material in the area of maximum stress, resulting in the establishment of a relatively extensive field of residual stresses.

A series of electrical strain gauges (measurement base: 0.6 and 1.5 mm) positioned as shown in Fig. 3 was used to detect residual strains.

Total strain under no load, maximum load and half-load was determined during a cycle so as to obtain the value of $\Delta\varepsilon p$, i.e. the difference between strains during loading and unloading when the half-maximum load is

applied, as illustrated in fig. 4.
The elastic component is:

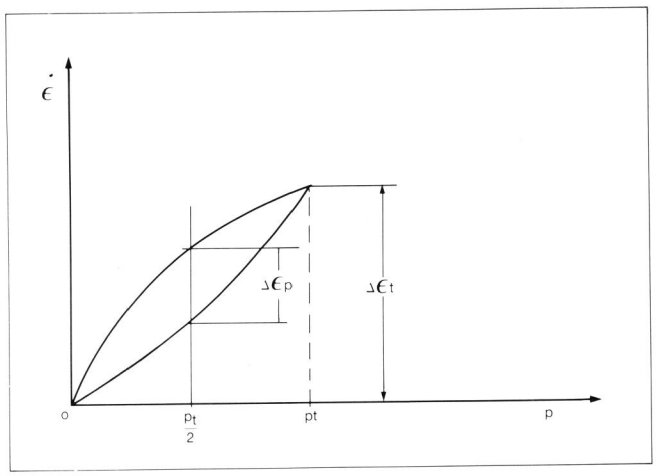

Fig. 4 - Pattern during a loading cycle.

It should be noted that the cyclic curve $\sigma-\varepsilon$ for SA 533 may rise to the residual stress value, since its peak corresponds to deformation equal to the sum of the residual deformation $\Delta\varepsilon_2$ and the total deformation $\Delta\varepsilon_t$.

This value is used to trace a line parallel to the elastic segment of the curve (see Fig. 5).

The value assigned to $\Delta\varepsilon_r$ is equal to the ordinate for $\varepsilon_2 + \Delta_{ep}$ on the parallel line. The Baushinger effect is ignored.

Fig. 5 - Scheme for calculating the residual σ_r.

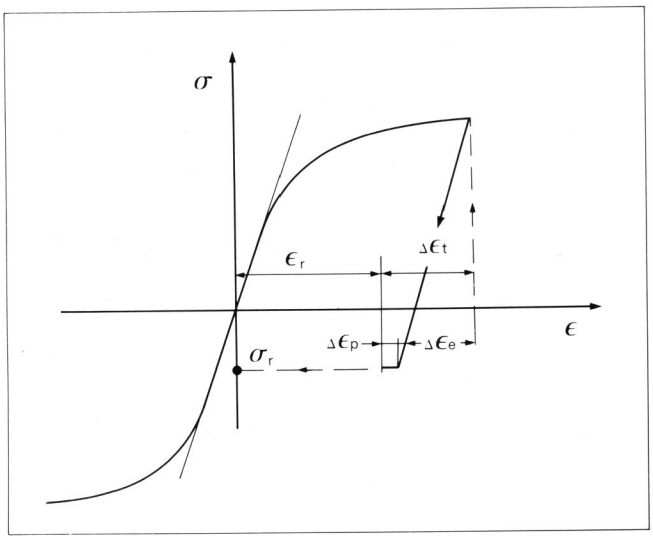

Residual stresses were measured after the first loading and then at constant load cycle intervals until crack nucleation.
The value of the internal stresses increased in function of the number of cycles, resulting in a continuous increase in the mean strain.

The residual stress pattern and values of nucleation are indicated in Fig. 6.

The specimens with holes were subjected to loads of 1250 to 12,500 (R = 0.1 as before). Once again, the da/dn trend was evaluated in function of ΔK with the Paris equation, using the same test procedure as for the specimens without holes.

Fig. 6 - Pattern of the residual stresses on the surfaces of the test specimens.

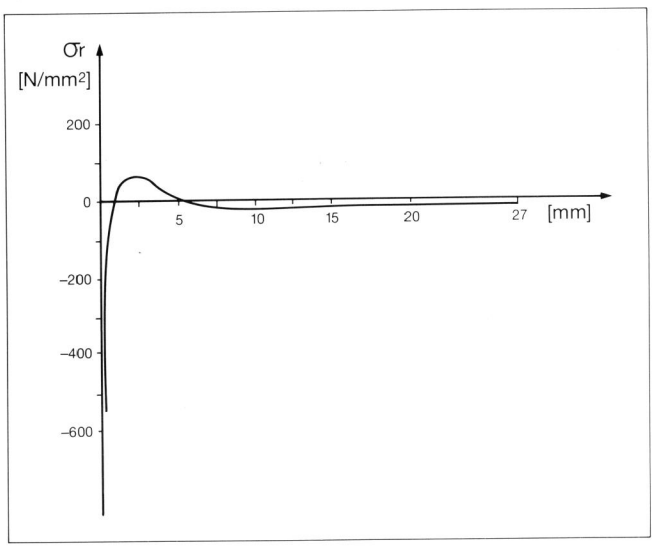

Experimental and theoretical results

Account must be taken of the presence of internal stresses when assessing the growth rate of a crack in function of ΔK.

The approach adopted in this study was to superpose intensity factors K_a and K_r corresponding to the applied and the residual stresses respectively, so as to obtain an effective intensity factor $K_{eff} = K_a + K_r$.

Since the internal stress pattern is known, the magnitude of K_r was determined by using its expression (8) in a notched specimen (see Fig. 7), with

a force acting on a point of one face of the crack:

$$K_I = \frac{2P}{\sqrt{\pi a}} F\left(\frac{c}{a}, \frac{a}{w}\right)$$

where:

$$F\left(\frac{c}{a}, \frac{a}{w}\right) = \frac{3{,}52\left(1 - \frac{c}{a}\right)}{\left(1 - \frac{a}{w}\right)^{\frac{3}{2}}} -$$

$$- \frac{4{,}35 - 5{,}28\,\frac{c}{a}}{\left(1 - \frac{a}{w}\right)^{\frac{1}{2}}} +$$

$$+ \left\{\frac{1.30 - 0{,}30\left(\frac{c}{a}\right)^{\frac{3}{2}}}{1 - \left(\frac{c}{a}\right)^{2}} + 0{,}83 - 1{,}76\,\frac{c}{a}\right\}$$

$$\left\{1 - \left(1 - \frac{c}{a}\right)\frac{a}{w}\right\}$$

This equation has been used (11) to calculate K_r irrespective of their trend by replacing P with $\sigma_r(c)$ and integrating over the entire length of the crack, where $\sigma_r(c)$, dc is the value of the residual stresses:

$$K_r = \int_o^a \frac{2\sigma_r\, dc}{\sqrt{\pi a}} F\left(\frac{c}{a}, \frac{a}{w}\right)$$

Fig. 7 - Formula for calculation of the stress intensity factor of a specimen with a single notch and a force acting on the face of the crack.

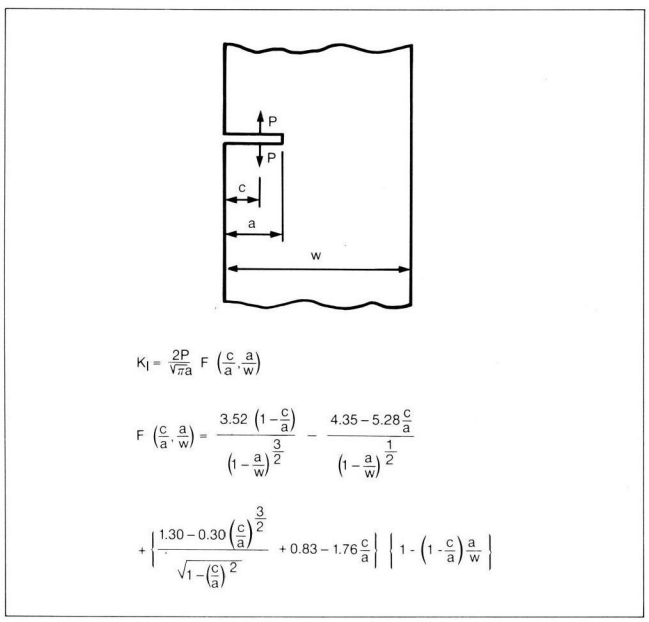

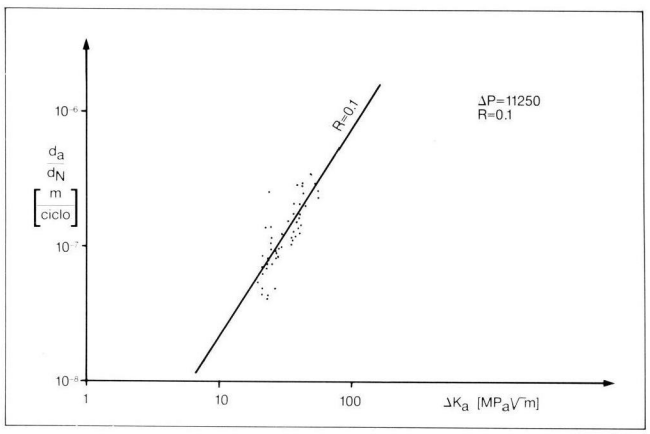

Fig. 8a - Trend of da/dN versus Ka (applied stresses intensity factor) derived from test specimens free from residual stresses.

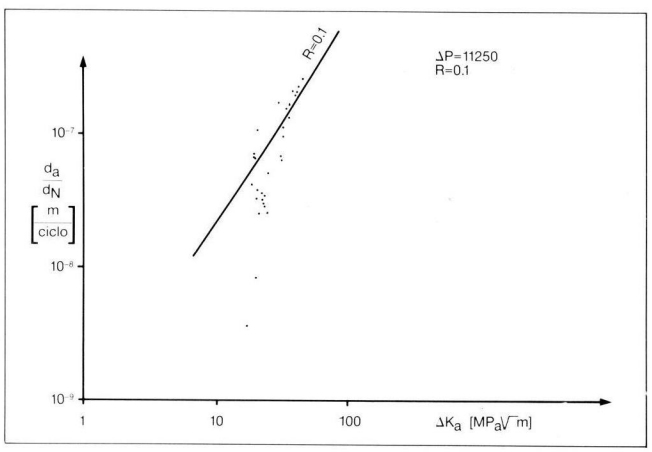

Fig. 8b - Trend of da/dN versus Ka (applied stresses intensity factor) derived from test specimens with residual stresses.

The integrations are performed numerically with a computer.
The trend of the da/dN curves versus K in the presence and the absence of residual stresses is illustrated in Fig. 8, while the trend of K_a and K_r (and hence of K_{eff}) is shown in Fig. 9.

The presence of residual stresses obviously alters R.

A ratio $R_{eff} = \frac{K_{eff\ min}}{K_{eff\ max}}$ was therefore determined, for

which $K_{eff} = 0$ when $K_{eff\ min}$ is $\leqslant 0$ (see Fig. 8).

Examination of Fig. 8 shows that when residual stresses are present the da/dN is initially below the characteristic curve determined with R = 0.1, whereas when the crack length is about 2.5 mm its growth rate

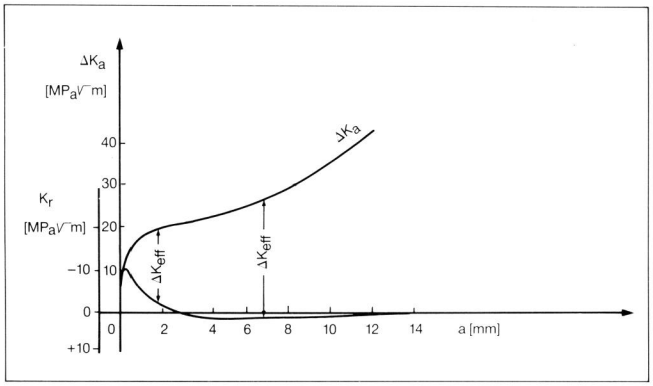

Fig. 9 - Trend of Ka (applied stresses intensity factor) versus crack length (a).

is slightly higher than that of the baseline. Figs. 9 & 10 make it clear that at this crack lenght, K_r changes signs and becomes positive due to the presence of internal stresses.

Fig. 10 - Trend of $K_{eff.\ max}$ (maximum effective stresses intensity factor) and $K_{eff.\ min}$ (minimum effective stresses intensity factor) and of $R_{eff} = K_{eff.\ min} / K_{eff.\ max}$.

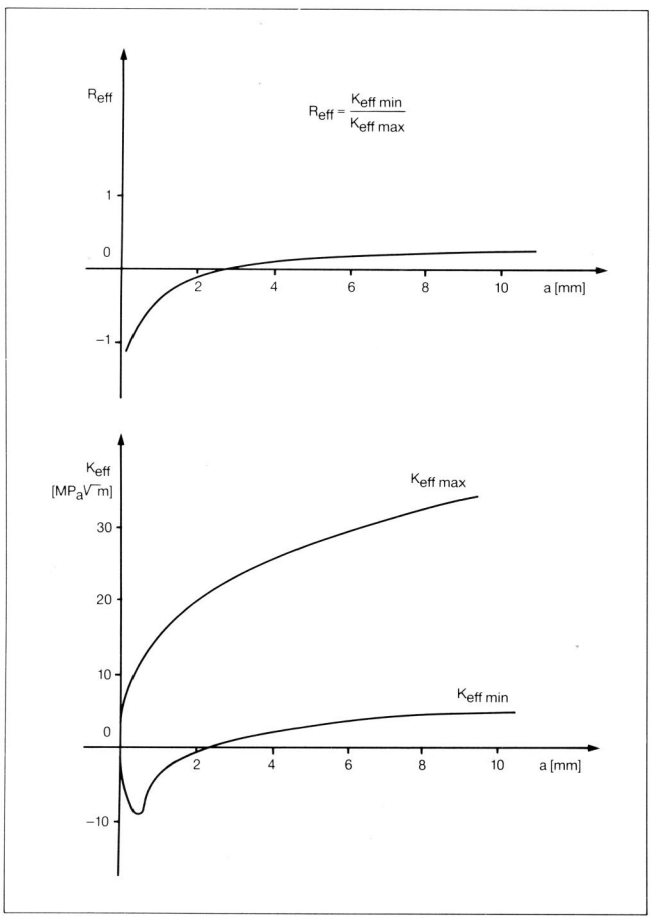

When the crack length is < 2.5 mm, therefore, K_r is negative and K_{eff} is less than Ka. This provides an explanation for the slowing down of the propagation rate observed experimentally. When the length is > 2.5 mm, K_r becomes positive and $\Delta K_{eff} = \Delta Ka$.

Accelerated propagation can be referred to a variation in R_{eff}, which changes from negative to positive as a result of the changes in the sign of K_r, and hence moves away from the baseline.
Fig. 11 shows the experimental and theoretical trend of da/dN versus ΔK_a the latter being calculated from:

$$\frac{da}{dN} = C(\Delta K_{eff})^n$$

where the values for C and n are those for the specimens without holes: $C = 6.555.10^{-9}$; $n = 1.52$.

Neither curve follows the Paris equation pattern. Both, in fact, display a sharp change in tangent at crack length a = 2.5 mm, i.e. the value at which K_r and R_{eff}, change sign.

Internal stresses thus influence the growth rate and hence the propagation of a fatigue crack. Initially, in fact, there is a marked slowing down. Then as K_{eff} and R_{eff} approach zero, the effect of the residual stresses diminishes. K_{eef} and R_{eff} become positive and the crack growth rate increases.

Calculation of an effective intensity factor is an efficacious way of explaining the experimental picture. The change in da/dN versus K_a curve, as the crack moves into zones with residual stresses of different

Fig. 11 - Trend of da/dN versus Ka (applied stresses intensity factor), both experimental and theoretical), in the presence of internal stresses. The theoretical curve is calculated from $da/dN = C\ (K_{eff})^n$.

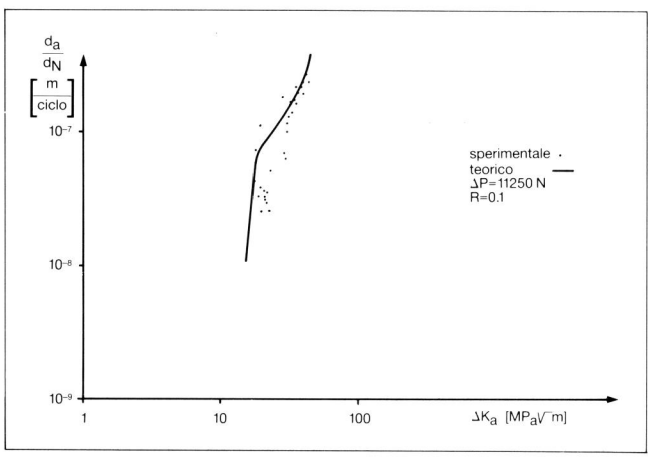

sign reported by other workers (3,4), on the other hand, was not observed.

At all events, it is considered that the field of internal stresses changes so as to maintain the condition at zero resultant and moment.
The trend for a versus N is illustrated for both types of test specimen in Fig. 10, which illustrates the effect of internal stresses on fatigue life.

The nucelation time of specimens with residual compression stresses at their tip is more than twice that of specimens with no residual stresses. The time of propagation is slightly shorter when internal stresses occur.

Fig. 12 - Crack length a versus N (no. of load cycles).
a) specimens without residual stresses b) specimens with residual stresses.

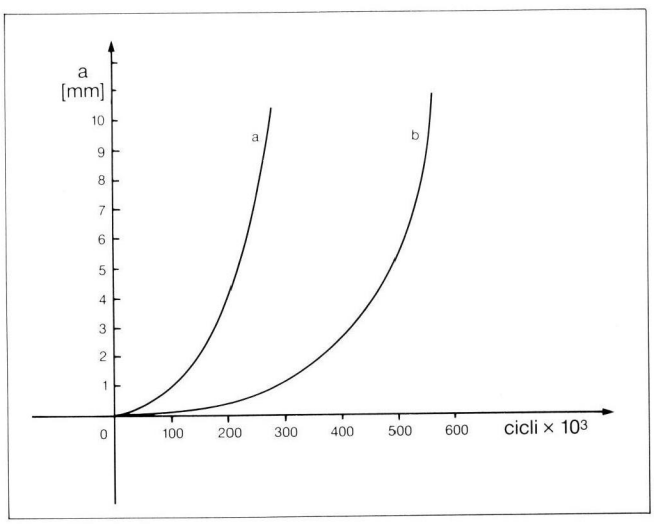

Conclusions

The results of this study offer further evidence of the substantial influence exerted by residual stresses on the growth rate of fatigue cracks.

A careful estimate, however, must be made of the residual stresses and their corresponding stress intensity factor must be correctly evaluated when making a crack growth rate prediction.

A good fit between the experimental results and the theoretical predictions was obtained in this work by calculating the self-stresses due to local plasticisation, and by using the superposition of intensity factors approach.

There was a significant variation in the influence of residual stresses: initially compression stresses with negative K_r values, are present at the tip, and after penetrating with positive K_r values.

The influence of the change in sign of the field of internal self-stresses observed at the tip by other works and attributed (12) to the re-equilibrium of such stresses as the crack advances, on the other hand, was not noted in this study.

It may be remarked that changes in the value of K_r also alter the value of R_{eff}, resulting in a further shift away from the baseline.
This work was supported by Ministry of Education 60% and 40% Grant 1983/84.

Annex A

Given an expression for the stresses-cyclic deformation law of the type an taking the total strain as:

$$\sigma = K' (\varepsilon_p)^{n'}$$

$$\varepsilon_t = \varepsilon_e + \varepsilon_p = \frac{\sigma}{E} + \left(\frac{\sigma}{K'}\right)^{1/n'}$$

one can calculate the cyclic $\sigma(\varepsilon)$ curve of the material. The literature (10) offers the following K′ and n′ values for materials with mechanical characteristics similar to those of SA 533:

K′ = 1379 MPa
n′ = 0.15

A value for εp is provided by:

$$\varepsilon_p = \left(\frac{\sigma}{K'}\right)^{1/n'}$$

from which σ is derived, and hence ε_c. The sum of ε_p + ε_t is equal to ε_t.

ε_p [%]	0	0,1	0,2	0,5	1	2
σ [MPa]	0	489	543	623	691	767
ε_e [%]	0	0,23	0,26	0,30	0,33	0,37
ε_t [%]	0	0,33	0,46	0,80	1,33	2,37

The material is assumed to display a symmetrical behaviour on compression.